Hindawi
International Journal of Photoenergy
Volume 2018, Article ID 4954039, 8 pages
https://doi.org/10.1155/2018/4954039

Research Article

Photocatalytic Degradation and Hydrogen Production of TiO_2/Carbon Fiber Composite Using Bast as a Carbon Fiber Source

Guomei Tang,[1,2,3] **Asim Abas**,[1] **and Shanpeng Wang**[1]

[1]*School of Physical Science and Technology, Lanzhou University, Lanzhou 730000, China*
[2]*School of Mathematics and Computer Science Institute, Northwest Minzu University, Lanzhou, Gansu 730030, China*
[3]*State Key Laboratory of Advanced Processing and Recycling of Non-Ferrous Metals, Lanzhou University of Technology, Lanzhou 730050, China*

Correspondence should be addressed to Guomei Tang; tanggm13@lzu.edu.cn

Received 17 January 2018; Accepted 10 April 2018; Published 3 June 2018

Academic Editor: Xuxu Wang

TiO_2/carbon fiber composite is achieved by loading TiO_2 nanoparticles on biomass carbon fiber, which originates from the carbonized natural bast. The carbonized process and the loading amount of TiO_2 are researched in detail. It is found that the carbonized bast fiber shows robust adsorption characteristics for TiO_2 nanoparticles in aqueous dispersion, and TiO_2 nanoparticles with ~15 wt.% in total weight are uniformly loaded onto the fiber surface. The photocatalytic properties of TiO_2/carbon fiber composite are evaluated by photocatalytic degradation of rhodamine B and water splitting for hydrogen production. The results indicate that 90% RhB molecules could be attacked in 60 min under UV light irradiation, and the hydrogen production rate of water splitting is up to 338.51 μmol/h. The highlight is that TiO_2/carbon fiber composite is easy to be recycled due to the incorporation of macroscopical biomass carbon fiber.

1. Introduction

Since Fujishima and Honda reported the groundbreaking research work on splitting water to produce hydrogen on TiO_2 electrode [1], the photocatalysis had aroused great interest. TiO_2 nanomaterials possess commendable performance in terms of its nontoxic, cost effectiveness, strong oxidizing activity, and long-term stability against photocorrosion, which have a very broad application prospect in many fields, such as air pollution, waste water treatment, hydrogen production, and sterilization [2–7]. The application of TiO_2 nanomaterials is greatly limited due to the poor visible light response and high charge recombination rate, originating from the wide band gap (3.2 eV for anatase and 3.0 eV for rutile) and the relatively high electrical resistance. TiO_2 is combined with carbon species such as carbon nanotubes, graphene, carbon fiber, and graphite-like carbon to form TiO_2/carbon composites [8–12] due to the good adsorbability and strong charge transport ability [13, 14].

Carbon fiber is a kind of one-dimensional carbon material with excellent properties, such as high tensile strength, low weight, high chemical resistance, high temperature tolerance, and excellent electrical conductivity, making them very popular in many fields. However, commercialized carbon fiber is relatively expensive due to the raw materials and fabrication process, which is not conducive to the photocatalyst application in the wide range. Biomass fiber carbonization is a feasible route to obtain low-cost carbon fiber, which can meet some applications with no high requirement on mechanical behavior, such as photocatalyst and solar cells.

In the liquid phase system, TiO_2 nanomaterials are difficultly recycled after reaction; the poison and aggregate of TiO_2 powder are also disadvantageous factors [15]. They all seriously restrict the practical application of photocatalysis. Therefore, it is an effective way to solve the recovery of photocatalyst by combining TiO_2 nanomaterials with carbon fiber.

Natural bast fiber was used in textile in the ancient times. Its main component is cellulose, which takes up about 75% content of the fiber. The bast becomes a kind of high-

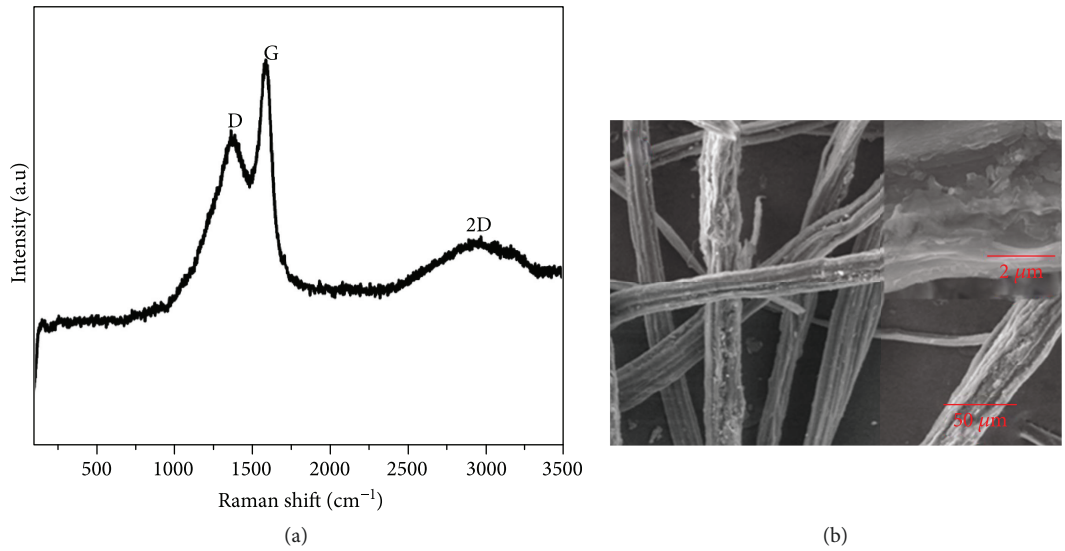

Figure 1: The Raman spectrum (a) and SEM image (b) of biomass carbon fiber.

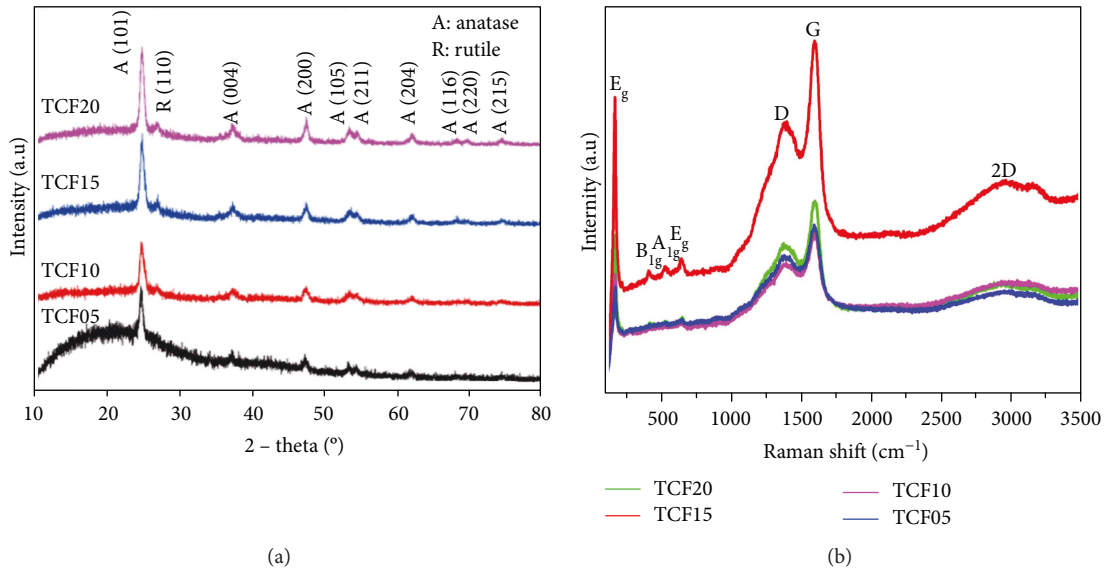

Figure 2: XRD patterns (a) and Raman spectra (b) of TiO_2/carbon fiber micronanocomposites.

strength, low elongation fiber, so it is an ideal raw material of biomass carbon fiber. However, the electrical conductivity, high temperature resistance, and the chemical and physical adsorptions of bast fiber are disadvantageous. Biomass fiber carbonization is a suitable way to improve electrical conduction and structural properties, including increasing porous structure and fiber roughness, which are conducive to enhance the adhesion and load amount of TiO_2 nanomaterials on the surface of biomass carbon fiber. Because bast fiber is widely accessible and low cost, the biomass carbon fiber using bast fiber as a raw material has great advantages in practical application of catalyst carrier.

Here, the bast was carbonized to get biomass carbon fiber. Then, the carbon fiber was put into TiO_2 nanoparticle dispersion with different concentrations to obtain optimal TiO_2/carbon fiber composite. Using the recycled photocatalyst, the photocatalytic degradation of rhodamine B (RhB) and water splitting for hydrogen production were performed, 90% RhB molecules were attacked in 60 min under UV light irradiation, and the hydrogen production rate was up to 338.51 μmol/h. A theoretical model was proposed to explain the photocatalytic mechanism of the composites.

2. Experimental Section

2.1. Preparation of the Sample. TiO_2/carbon fiber composites were prepared by the following process. A certain amount of bast fiber was located into the tube furnace. In the hydrogen ambience with 100 sccm, the fiber was heated to 300°C at a rate of 10°C/min and then maintained for 1.5 h. The biomass

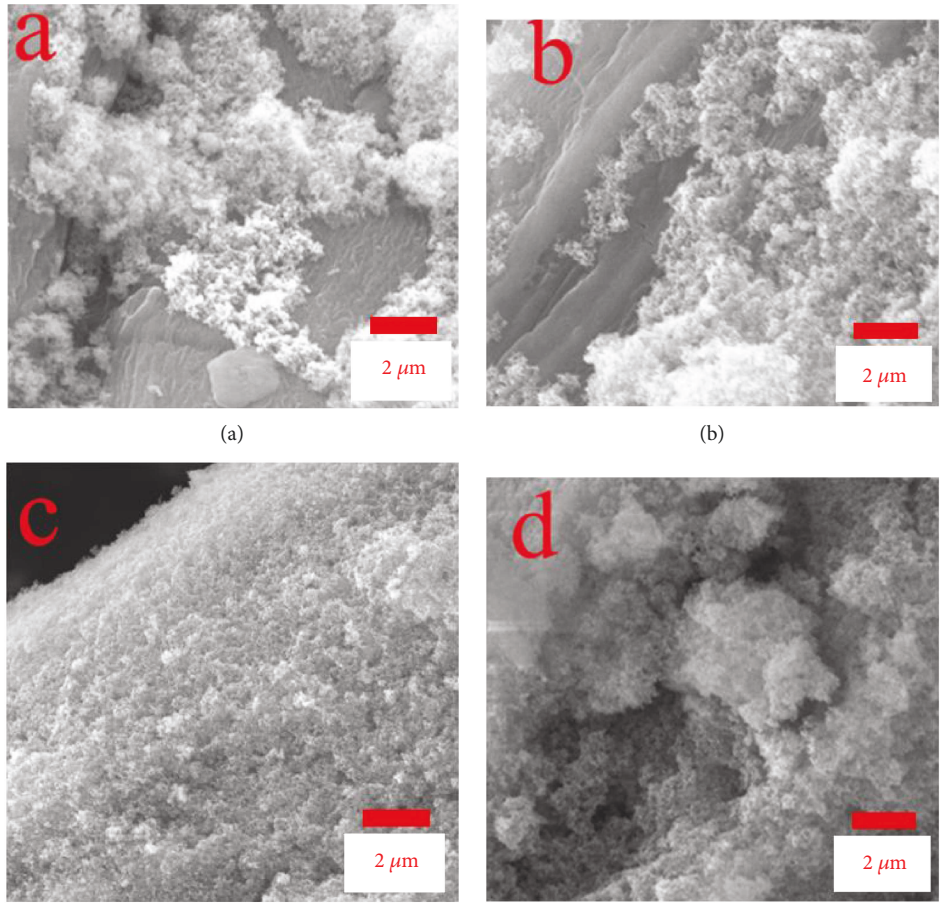

(a) (b)

(c) (d)

Figure 3: (a–d) SEM images of TCF05, TCF10, TCF15, and TCF20.

carbon fiber was obtained after cooling down. Different amounts of TiO_2 nanoparticles (P25) were dispersed into 50 mL deionized water with strong ultrasonic to attain homogenous dispersion (5, 10, 15, and 20 g/L, resp.). After immersing the biomass carbon fiber into TiO_2 dispersion for several minutes, the composites were annealed at 450°C under H_2 ambience. TiO_2/carbon fiber composites with different concentrations of TiO_2 dispersions, labelled as TCF05, TCF10, TCF15, and TCF20, could be achieved by repeating the above-depicted procedures to increase the load amount. The load amount of TiO_2 nanoparticles was estimated to be about 15 wt.% in total mass.

2.2. Characterization. The morphology of the samples was characterized by field emission scanning electron microscopy (FESEM, Hitachi S4800). Raman spectroscopy (Horiba Jobin Yvon LabRAM HR800) and grazing-angle X-ray diffraction (Rigaku D/MAX-2400) were employed to characterize the crystal structure of the samples. UV-visible absorption spectrum was recorded using Hitachi U-3900H spectrophotometer to evaluate the photocatalytic degradation performance. Water splitting for hydrogen production was applied to evaluate the photocatalysis on photocatalytic hydrogen production system (Labsolar-IIIAG, Perfectlight Technology Co. Ltd., China).

2.3. Photocatalytic Activity Test

2.3.1. Photocatalytic Degradation of RhB Molecules. The photocatalytic activities were evaluated by photodegradation of RhB molecules. The procedures had been reported in the previous works [16–18]. 0.2 g TiO_2/carbon fiber composite was dispersed into 100 ml RhB solution (10 mg/L). The suspensions were magnetically stirred in dark for 30 minutes to reach the adsorption-desorption equilibrium. The degradation was carried out under high pressure xenon lamp (300 W) with a cutoff filter ($\lambda \geq 400$ nm). During the irradiation, 4.5 ml dispersion was collected and centrifuged to remove the catalysts with a time interval. The filtrates were analyzed by recording the changes of the absorption bands (around 554 nm) of RhB using Hitachi U-3900H spectrophotometer. After the photocatalyst reaction, TiO_2/carbon fiber composite was rinsed by ethanol and deionized water and dried for recycling.

2.3.2. Photocatalytic Hydrogen Production from Water Splitting. 0.15 g TiO_2/carbon fiber composite was added into

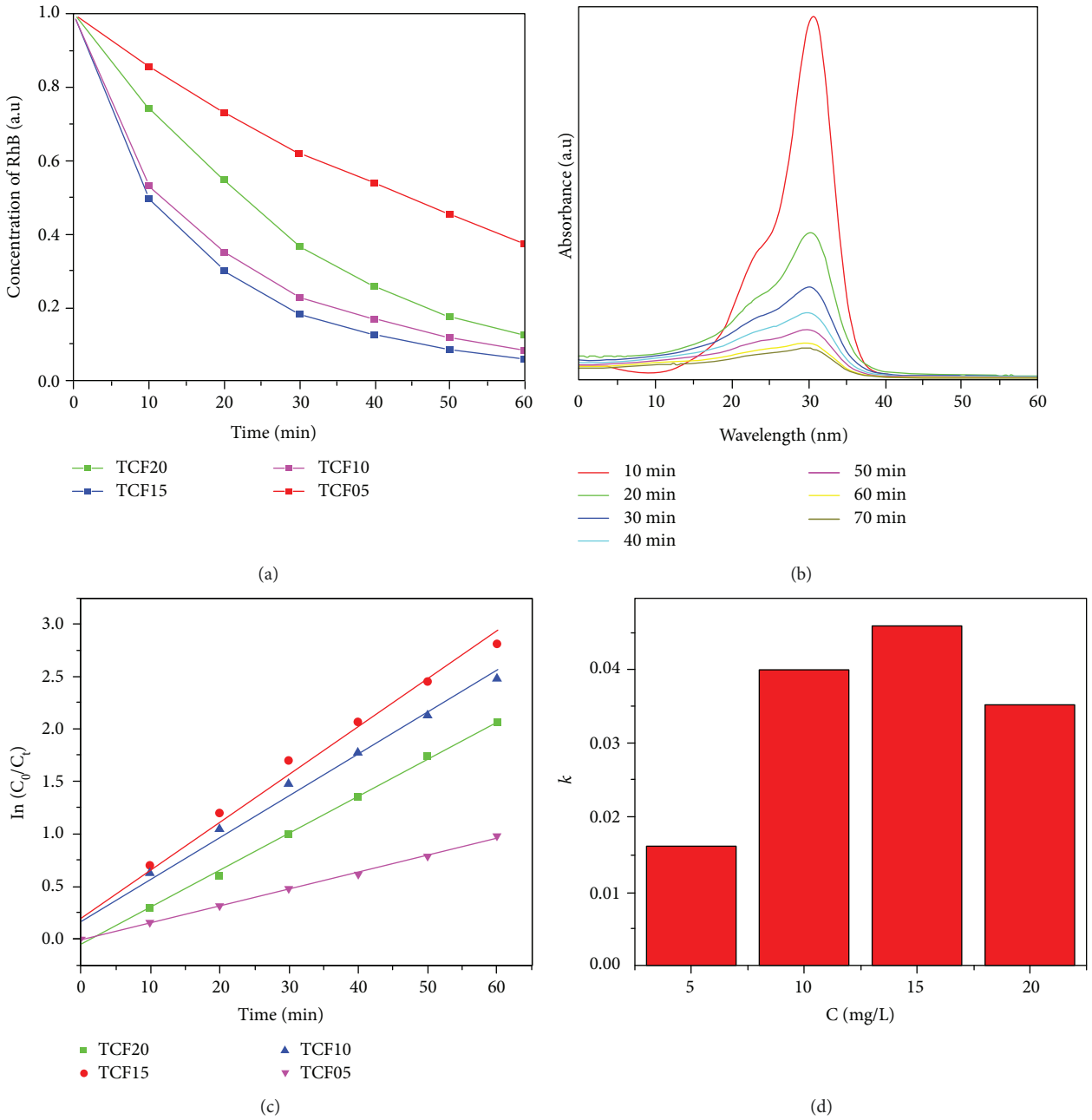

FIGURE 4: (a) The photocatalytic degradation of RhB with different TiO_2/carbon fiber micronanocomposites under UV light irradiation. (b) Absorption spectral changes of RhB solution under UV light irradiation in the presence of TCF15. (c) The degradation kinetic data of RhB under UV light irradiation at different sampling time (d). Degradation rate K value of different samples.

the solution mixed by 90 ml water and 10 ml methanol. 2.5 uL chloroplatinic acid solution (10 mg/L), as the assistant catalyst, was added into the solution. Under the 300 W xenon lamp (with cutoff filter) irradiation, the hydrogen amount was analyzed by gas chromatography (GC 7900).

3. Results and Discussion

Figures 1(a) and 1(b) are Raman and SEM images of biomass carbon fiber. Figure 1(a) shows that D peak and G peak of the biomass fiber were located at around 1360 cm^{-1} and 1580 cm^{-1}, which are consistent with the Raman shift peaks of carbon [19]. This indicates that natural bast fiber has been transformed into inorganic carbon fiber after 300°C carbonization process in hydrogen ambience. Figure 1(b) shows that the surface of carbon fiber is much rough. There is a lot of hollow structure on the surface of biomass carbon fiber (the inset), which is in favor of enhancing the adhesion and loading amount of TiO_2 nanoparticles on carbon fiber. In addition, during the measurement process of SEM images, we find that the electrical conduction of the biomass carbon fiber is obviously good,

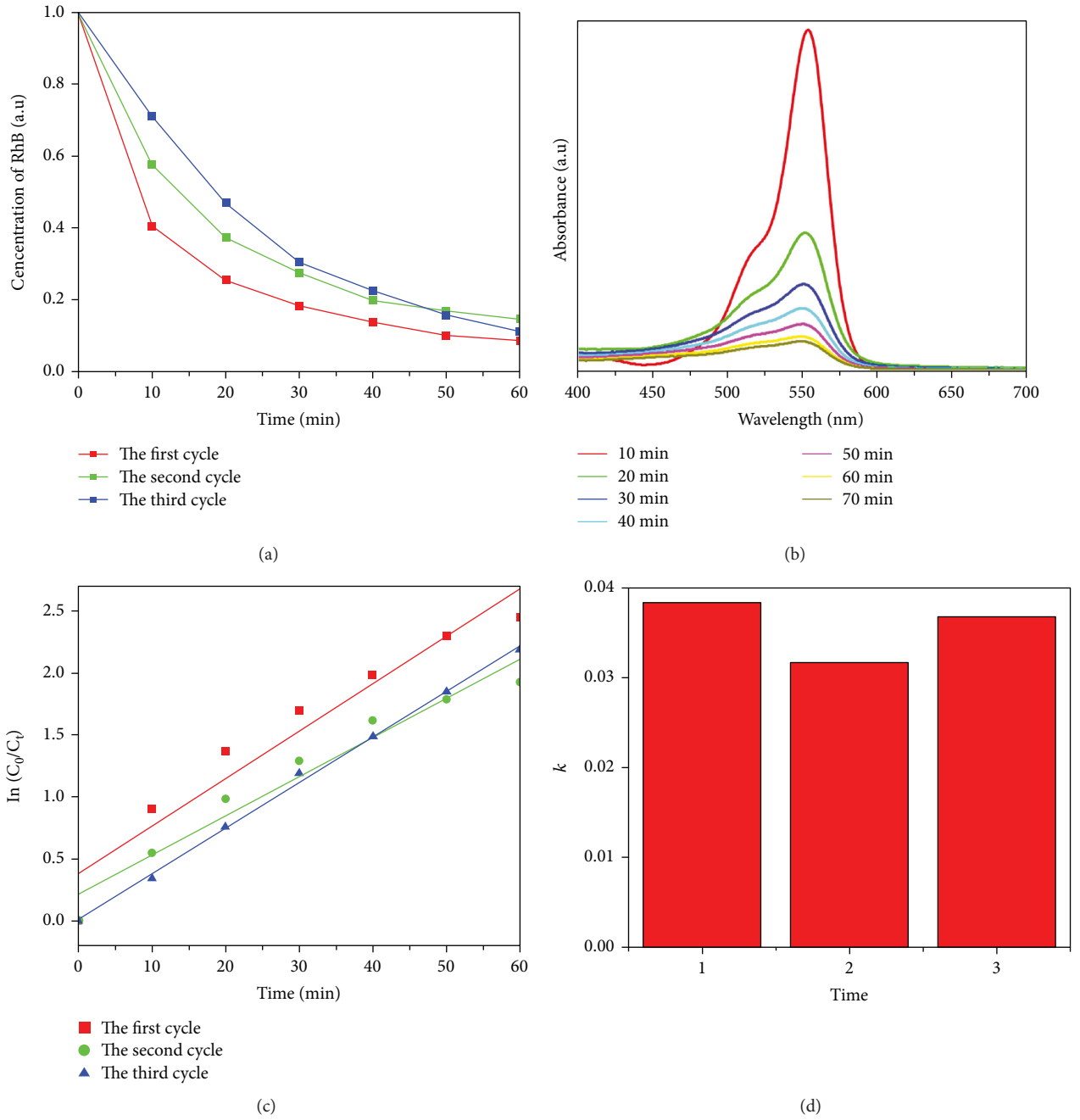

Figure 5: (a) The cycle test of TCF15 for photocatalytic degradation of RhB under UV light irradiation. (b) Absorption spectral changes of RhB solution under UV light irradiation in the presence of TCF15. (c) The degradation kinetic data of RhB under UV light irradiation at different cycle times. (d) Degradation rate K value data calculated from (c).

which facilitates the photocatalytic activity of TiO_2/carbon fiber composite.

Figure 2 is XRD patterns and Raman spectra of TCF05, TCF10, TCF15, and TCF20 samples. In Figure 2(a), the peaks sited at approximately 25.21, 37.81, 47.81, 53.91, 55.11, 62.81, 68.81, 70.51, 75.31, and 27.48° are corresponding to the crystal plane (101), (004), (200), (105), (211), (204), (116), (220), and (215) of anatase TiO_2 and (110) of rutile TiO_2, respectively. The broad diffraction peak located at around 20° is related to amorphous carbon, and the peak gradually decreases due to the increase of TiO_2 load amount from TCF05 to TCF20. These results indicate that the loaded photocatalyst on the biomass carbon fiber is a mixture of anatase and rutile TiO_2. Figure 2(b) shows the Raman spectra of TiO_2/carbon fiber composites. Besides the peaks of carbon fiber, the Raman shift peaks located at 144, 400, 518, and 640 cm^{-1} are related to the Eg, B1g, A1g, and Eg Raman vibrations of anatase TiO_2. It illustrates that there are a large number of TiO_2 nanoparticles on the biomass carbon fiber, which is consistent with XRD results.

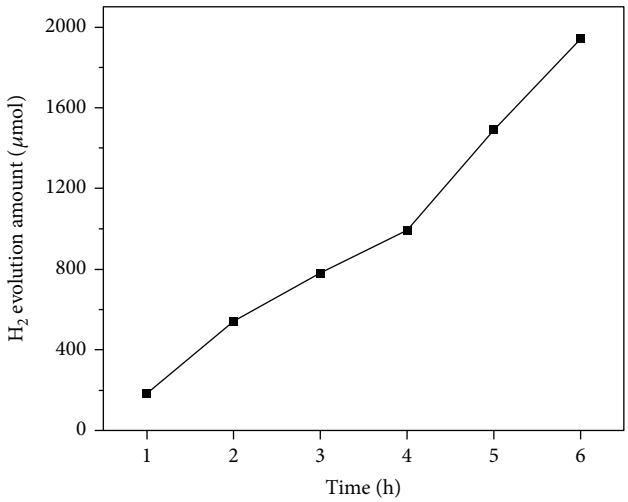

Figure 6: The hydrogen production of the TCF15 under UV light irradiation.

We can believe that TCF15 might be better in the four different TiO_2/carbon fiber composites based on the XRD and Raman spectra.

Figure 3 shows the SEM images of TCF05, TCF10, TCF15, and TCF20. For the TCF05 (Figure 3(a)) and TCF10 (Figure 3(b)), TiO_2 nanoparticles are locally adhered on the surface of biomass carbon fiber. After increasing TiO_2 dispersion concentration, the load amount of TiO_2 nanoparticles has been greatly improved for the TCF15 (Figure 3(c)). However, the exceeded dispersion concentration leads to the aggregation of TiO_2 nanoparticles on the biomass carbon fiber (Figure 3(d)). Due to the weak adhesion between TiO_2 nanoparticles, the aggregated nanoparticles will break off during the following photocatalysis experiment. Therefore, it is obvious that the optimal TiO_2/carbon fiber composite is TCF15 due to the suitable load amount and uniformity of TiO_2 nanoparticles.

Figure 4 shows the photocatalytic degradation of RhB molecules operated by TiO_2/carbon fiber composite under UV light irradiation. It can be seen that the TCF15 has the optimal photocatalytic efficiency from Figure 4(a). Photocatalytic reaction kinetic process should conform to the Langmuir-Hinshelwood model [20]:

$$-\frac{dC}{dt} = v = kH = kK[C](1 + K[C]). \quad (1)$$

Here, C is the concentration of RhB and K is a constant. When the initial concentration of reactants is low, the formula can make the appropriate mathematical transform:

$$\mathrm{Ln}\left(\frac{C_D}{C}\right) = Kt. \quad (2)$$

Here, C_0 represents the initial concentration of RhB and C is the concentration of RhB after irradiation t min. This formula is a reaction kinetic equation. It is found that TiO_2 photocatalytic degradation reactions abide by the first-order reaction kinetic equation [21, 22]. Based on the kinetic data in Figures 4(c) and 4(d), we can get the optimum load amount of TiO_2 nanoparticles on the TiO_2/carbon fiber composites by comparing the degradation rate K value. It is obviously seen that TCF15 is the optimal composites in our research range. TiO_2 nanoparticles are uniformly loaded on the TCF15 surface, and an ideal photocatalytic efficiency can be expected. The higher concentration will lead to the aggregation of TiO_2 nanoparticles and the exfoliation in the photocatalyst experiment process.

To characterize the stabilization of the photocatalysis properties, TCF15 is done in the cycle test for photocatalytic degradation of RhB molecules (Figure 5). It can be seen that the photocatalyst efficiency of TCF15 has no obvious decrease after three cycles. The degradation of RhB molecules was more than 90% within 60 min. Therefore, the composite maintains the high photocatalytic degradation performance. It indicates that the TiO_2/carbon fiber composite has the reusability without the decrease of photocatalysis efficiency.

Besides the photocatalytic degradation of organic molecules, water splitting for hydrogen production is another excellent property of photocatalyst. The TiO_2/carbon fiber composite can also be used to produce hydrogen energy. Figure 6 shows the photocatalytic hydrogen production under UV light irradiation with TCF15. It is found that the amount of production hydrogen with TCF15 photocatalyst linearly increases with the increase of irradiation time. The average hydrogen production rate reaches to 338.51 μmol/h. Therefore, we believe that the TiO_2/carbon fiber composite not only has superior photocatalytic degradation reusability, but also exhibits excellent photocatalytic hydrogen production performance.

The above-depicted results indicate that TiO_2/carbon fiber composite has the superior photocatalytic degradation of RhB molecules and water splitting for hydrogen production. To check the reliability of the composite, XRD and SEM are carried out on the TCF15 sample after performing the photocatalysis experiments. In Figure 7(a), the XRD peaks of TiO_2 are still very obvious, which indicate that TiO_2 nanoparticles existed after photocatalytic reaction. SEM image (Figure 7(b)) also proves that the TiO_2 nanoparticles are still uniformly loaded on the surface of carbon fibers, which indicates that the exfoliation of TiO_2 nanoparticle is not obvious.

Based on the above experimental results, a model is proposed to explain the photocatalytic mechanism of TiO_2/biomass carbon fiber composite. Figure 7(c) shows the schematic diagram of the photocatalysis. The biomass carbon fiber surface is very rough, and there is a large number of hollow structures with robust physical adsorption characteristics. After loading TiO_2 nanoparticles, the roughness of the fibers is further increased, which is beneficial to the absorption of RhB molecules. As seen from Figure 2(a), TiO_2 nanoparticles are made of anatase and rutile phases with 80 : 20 ratio, which formed the heterojunctions (the schematic diagram in Figure 7(d)) [23]. Under the UV light irradiation, the electrons are excited from the valance band (E_v) into the conduction band (E_c) in TiO_2, leaving the holes in the valance band. Due to the separation effect of TiO_2 heterojunctions for the photogenerated electron-hole pairs, the

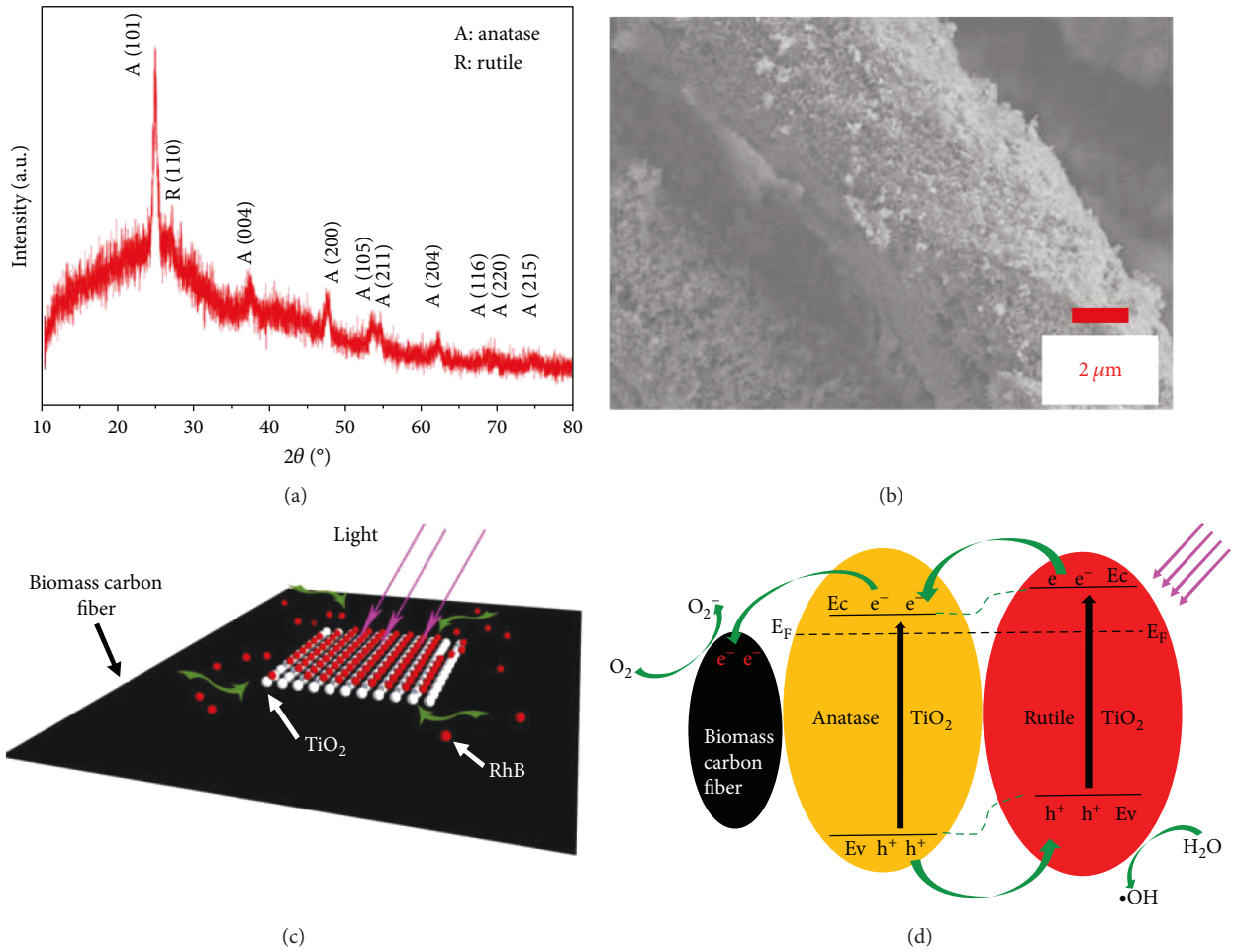

FIGURE 7: XRD pattern (a) and SEM (b) image of TCF15 after the photocatalytic degradation cycle. (c, d) Photocatalytic reaction mechanism diagram.

photogenerated electrons would transfer from the excited rutile TiO_2 phase to the E_c band of anatase TiO_2 phase. At the same time, the photogenerated holes would collect in the E_v band of rutile TiO_2 phase. It is noted that TiO_2 heterojunctions are loaded on the surface of carbon fibers. The carbon fibers have the ability of electron capture since they show high electron storage capacity and electrical conductivity [24]. Due to lower Fermi level of carbon fibers than that of anatase TiO_2 phase, electrons transferred from anatase TiO_2 phase to carbon fibers can be prompted. The above-depicted two processes can minimize the recombination chance of the photogenerated electron-hole pairs, which improves the efficiency of the photocatalytic activity. After being separated, the photogenerated holes combine with water molecules to form hydroxyl radicals. Meanwhile, superoxide radicals can be formed by combining the photogenerated electrons with oxygen molecules. These radicals possess the potential to oxidize the adsorbed RhB molecules on the photocatalyst surfaces [25]. Photocatalytic degradation process of RhB molecules is dominated by the oxidation of chemical reaction under the UV light irradiation. In addition, the strong adsorption ability of carbon fibers increases the contact opportunities of RhB molecules with the composites, which are also beneficial to the enhancement of photocatalytic properties. Photocatalytic hydrogen production is a dominant reduction reaction of water splitting. Methanol is used to consume the photogenerated hole carriers. The electrons reduce water molecules to produce hydrogen. Therefore, through the design of micronanostructure, we have achieved the recycled, high-efficient TiO_2/biomass carbon fiber composite photocatalyst.

4. Conclusions

As the raw material, natural bast fiber is carbonized to get biomass carbon fiber. TiO_2/carbon fiber composites are achieved by combining biomass carbon fiber and TiO_2 nanoparticles with anatase and rutile mixed phase. Based on the superior adsorbability and electrical conduction of the biomass carbon fiber, the composites show the excellent catalytic activities on photocatalytic degradation and water splitting for hydrogen production. The rate of photocatalytic hydrogen production can reach 338.51 μmol/h. The very favorable feature for TiO_2/carbon fiber composite is easy to recycle as the photocatalyst.

Data Availability

The data used to support the findings of this study are available from the corresponding author upon request.

Conflicts of Interest

The authors declare that they have no conflicts of interest.

Acknowledgments

This work was supported by a grant from the Fundamental Research Funds for the Central Universities (Grant no. 31920170036) and the State Key Laboratory of Advanced Processing and Recycling of Non-Ferrous Metals, Lanzhou University of Technology (SKLAB02014003).

References

[1] A. Fujishima and K. Honda, "Electrochemical photolysis of water at a semiconductor electrode," *Nature*, vol. 238, no. 5358, pp. 37-38, 1972.

[2] M. Choi, J. Lim, M. Baek, W. Choi, W. Kim, and K. Yong, "Investigating the unrevealed photocatalytic activity and stability of nanostructured brookite TiO_2 film as an environmental photocatalyst," *ACS Applied Materials & Interfaces*, vol. 9, no. 19, pp. 16252–16260, 2017.

[3] J. Yao and C. Wang, "Decolorization of methylene blue with TiO_2 sol via UV irradiation photocatalytic degradation," *International Journal of Photoenergy*, vol. 2010, Article ID 643182, 6 pages, 2010.

[4] G. Yi, B. Xing, J. Jia et al., "Fabrication and characteristics of macroporous TiO_2 photocatalyst," *International Journal of Photoenergy*, vol. 2014, Article ID 783531, 7 pages, 2014.

[5] Q. Sun, Y. Lu, J. Tu, D. Yang, J. Cao, and J. Li, "Bulky macroporous TiO_2 photocatalyst with cellular structure via facile wood-template method," *International Journal of Photoenergy*, vol. 2013, Article ID 649540, 6 pages, 2013.

[6] A. Nishimura, N. Ishida, D. Tatematsu et al., "Effect of Fe loading condition and reductants on CO2 reduction performance with Fe/TiO_2 photocatalyst," *International Journal of Photoenergy*, vol. 2017, Article ID 1625274, 11 pages, 2017.

[7] Z. Fang, Y. Wang, D. Xu, Y. Tan, and X. Liu, "Blue luminescent center in ZnO films deposited on silicon substrates," *Optical Materials*, vol. 26, no. 3, pp. 239–242, 2004.

[8] C. Zhu, B. Lu, Q. Su, E. Xie, and W. Lan, "A simple method for the preparation of hollow ZnO nanospheres for use as a high performance photocatalyst," *Nanoscale*, vol. 4, no. 10, pp. 3060–3064, 2012.

[9] L. Wang, L. Shen, Y. Li, L. Zhu, J. Shen, and L. Wang, "Enhancement of photocatalytic activity on TiO_2-nitrogen-doped carbon nanotubes nanocomposites," *International Journal of Photoenergy*, vol. 2013, Article ID 824130, 7 pages, 2013.

[10] L. C. Sim, K. H. Leong, S. Ibrahim, and P. Saravanan, "Graphene oxide and Ag engulfed TiO_2 nanotube arrays for enhanced electron mobility and visible-light-driven photocatalytic performance," *Journal of Materials Chemistry A*, vol. 2, no. 15, pp. 5315–5322, 2014.

[11] L. Ji, Y. Zhang, S. Miao, M. Gong, and X. Liu, "In situ synthesis of carbon doped TiO_2 nanotubes with an enhanced photocatalyticperformance under UV and visible light," *Carbon*, vol. 125, pp. 544–550, 2017.

[12] C. Chen, S. Cao, H. Long et al., "Highly efficient photocatalytic performance of graphene oxide/TiO_2-Bi_2O_3 hybrid coating for organic dyes and NO gas," *Journal of Materials Science: Materials in Electronics*, vol. 26, no. 6, pp. 3385–3391, 2015.

[13] Y. Cui, Q. Wei, H. Park, and C. M. Lieber, "Nanowire nanosensors for highly sensitive and selective detection of biological and chemical species," *Science*, vol. 293, no. 5533, pp. 1289–1292, 2001.

[14] A. K. Geim and K. S. Novoselov, "The rise of graphene," *Nature Materials*, vol. 6, no. 3, pp. 183–191, 2007.

[15] J. Yu, G. Wang, B. Cheng, and M. Zhou, "Effects of hydrothermal temperature and time on the photocatalytic activity and microstructures of bimodal mesoporous TiO_2 powders," *Applied Catalysis B: Environmental*, vol. 69, no. 3-4, pp. 171–180, 2007.

[16] P. Jing, W. Lan, Q. Su, M. Yu, and E. Xie, "Visible-light photocatalytic activity of novel $NiTiO_3$ nanowires with rosary-like shape," *Science of Advanced Materials*, vol. 6, no. 3, pp. 434–440, 2014.

[17] P. Jing, W. Lan, Q. Su, and E. Xie, "High photocatalytic activity of V-doped SrTiO3 porous nanofibers produced from a combined electrospinning and thermal diffusion process," *Beilstein Journal of Nanotechnology*, vol. 6, pp. 1281–1286, 2015.

[18] C. Zhu, Y. Li, Q. Su et al., "Electrospinning direct preparation of SnO_2/Fe_2O_3 heterojunction nanotubes as an efficient visible-light photocatalyst," *Journal of Alloys and Compounds*, vol. 575, pp. 333–338, 2013.

[19] A. E. Lewandowska, C. Soutis, L. Savage, and S. J. Eichhorn, "Carbon fibres with ordered graphitic-like aggregate structures from a regenerated cellulose fibre precursor," *Composites Science and Technology*, vol. 116, pp. 50–57, 2015.

[20] J. M. Herrmann, "Photocatalysis fundamentals revisited to avoid several misconceptions," *Applied Catalysis B: Environmental*, vol. 99, no. 3-4, pp. 461–468, 2010.

[21] D. Monllor-Satoca, R. Gomez, M. Gonzalez-Hidalgo, and P. Salvador, "The "direct-indirect" model: an alternative kinetic approach in heterogeneous photocatalysis based on the degree of interaction of dissolved pollutant species with the semiconductor surface," *Catalysis Today*, vol. 129, no. 1-2, pp. 247–255, 2007.

[22] G. Xue, H. Liu, Q. Chen, C. Hills, M. Tyrer, and F. Innocent, "Synergy between surface adsorption and photocatalysis during degradation of humic acid on TiO_2/activated carbon composites," *Journal of Hazardous Materials*, vol. 186, no. 1, pp. 765–772, 2011.

[23] B. Lu, C. Zhu, Z. Zhang, W. Lan, and E. Xie, "Preparation of highly porous TiO_2 nanotubes and their catalytic applications," *Journal of Materials Chemistry*, vol. 22, no. 4, pp. 1375–1379, 2012.

[24] J. Shi, J. Chen, G. Li, T. An, and H. Yamashita, "Fabrication of Au/TiO_2 nanowires@carbon fiber paper ternary composite for visible-light photocatalytic degradation of gaseous styrene," *Catalysis Today*, vol. 281, no. 3, pp. 621–629, 2017.

[25] T. An, L. Sun, G. Li, Y. Gao, and G. Ying, "Photocatalytic degradation and detoxification of o-chloroaniline in the gas phase: mechanistic consideration and mutagenicity assessment of its decomposed gaseous intermediate mixture," *Applied Catalysis B: Environmental*, vol. 102, no. 1-2, pp. 140–146, 2011.